

# Thieno–Pyrrole-Fused BODIPY Intermediate as a Platform to Multifunctional NIR Agents

Samuel G. Awuah,<sup>[a]</sup> Sushanta K. Das,<sup>[b]</sup> Francis D'Souza,<sup>[b]</sup> and Youngjae You\*<sup>[a]</sup>

**Abstract:** We report the synthesis, photophysical and electrochemical properties, and in vivo fluorescence imaging of a series of new thieno–pyrrole-fused near-infrared (NIR) BODIPY agents by using a versatile intermediate as a building block. The versatile thieno–pyrrole-fused BODIPY intermediate was rationally designed to bear bromo-substituents and absorb in the mid-red region (635 nm) to act as an organic electrophile for the development of NIR multifunctional agents. The use of subsequent palladium-catalyzed and nucleophilic substitution reactions af-

forded highly conjugated NIR BODIPYs. The novel BODIPYs exhibit long-wavelength absorptions in the NIR region (650–840 nm). The agents produce sharp fluorescence bands, and most of them display respectable quantum yields of fluorescence (0.05–0.87) useful for biomedical imaging, as demonstrated by in vivo imaging with **SBDPIR740**. Interestingly, a number of

**Keywords:** BODIPY • fluorescent probes • imaging agents • photosensitizers • singlet oxygen

agents in the series that are non-halogenated were reactive to O<sub>2</sub> at the triplet photo-excited state coupled with a favorable redox potential and decent fluorescence, and hence could be potential candidates for use as photosensitizers in fluorescence-guided photodynamic therapy. Furthermore, the synthetic approach allows further functionalization of the highly conjugated NIR BODIPYs to tune the excited states (PET, ICT) and to conjugate targeting moieties for enhanced biological applications.

## Introduction

Near infrared (NIR) dyes are the subject of intense research as a result of their useful applications, which extend beyond the limited applications of UV and visible light. These dyes have been used in photovoltaic and advanced optoelectronics,<sup>[1]</sup> photodynamic therapy (PDT), and non-invasive bioimaging<sup>[2]</sup> as well as in laser printers and digital copy machines.<sup>[3]</sup> In PDT and bioimaging, the long-wavelength absorbing chromophores may have the valuable advantage of deeper tissue penetration.<sup>[4,5]</sup> However, NIR dye development generally requires tedious multi-step synthesis, often resulting in low reaction yields, reactive intermediates, poor solubility, poor photostability, and limited functionalization.<sup>[6]</sup>

The 4,4-difluoro-4-bora-3a,4a-diaza-s-indacenes (BODIPYs) provide synthetic advantages in addition to their pho-

to-stability, sharp absorption and emission, high molar absorptivity properties, and facile tuning of excited states.<sup>[7,8]</sup> Chemical modifications to the dipyrromethene core as well as functionalization of the boron center and the *meso* positions make BODIPYs adaptable for numerous applications as protein labels, fluorophores,<sup>[9]</sup> photosensitizers for PDT including activatable forms,<sup>[10, 11]</sup> energy concentrators,<sup>[12]</sup> and chemosensors.<sup>[13]</sup> Despite the wide use of BODIPYs and their excellent photophysical properties, the development of NIR BODIPYs with absorption > 700 nm is still challenging,<sup>[14]</sup> especially within the region of 800–900 nm. Hence, it is critical to develop a versatile but robust synthetic route to attain desirable functionalized NIR BODIPY analogues. Our work reported herein puts BODIPY dyes with unique NIR absorption and emission within reach, thus opening up new opportunities for their applications.

The search for building blocks for NIR BODIPYs has been a center of research activity in recent years. A classical but relevant route is to obtain a halogenated BODIPY framework for further reaction toward extended conjugation (Figure 1). Approaches by Dehaen and Boen et al.<sup>[15–17]</sup> who synthesized *meso*-halogenated BODIPYs, and 3,5-dichloro- and 1,7-dibromo-substituted BODIPYs, respectively, and by Hao et al. who developed 3-chloro and 3,5-diiodo-substituted BODIPYs for S<sub>N</sub>Ar and palladium-catalyzed coupling reactions<sup>[18–24]</sup> pushed the new BODIPYs to the visible/far red region of the electromagnetic spectrum. Churchill and co-workers, Hao et al., and Ravikanth et al. addressed the issue of halogen regioselectivity in BODIPYs for use as major building blocks.<sup>[25–27]</sup> Ravikanth and co-workers synthesized

[a] Dr. S. G. Awuah, Dr. Y. You  
Department of Pharmaceutical Sciences  
University of Oklahoma Health Sciences Center  
1110 N. Stonewall Ave, Oklahoma City, OK 73117 (USA)  
Fax: (+1) 405-271-7505  
E-mail: youngjae-you@ouhsc.edu

[b] S. K. Das, Dr. F. D'Souza  
Department of Chemistry  
University of North Texas  
1155, Union Circle, #305070, Denton, TX 76203-5017 (USA)  
Fax: (+1) 940-565-4318

Supporting information for this article is available on the WWW under <http://dx.doi.org/10.1002/asia.201300855>.

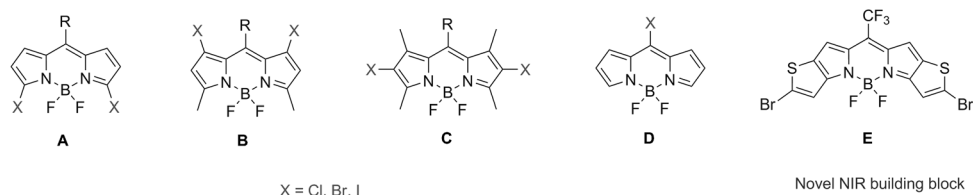


Figure 1. Chemical structures of BODIPY building blocks.

polyarylated BODIPYs using hexabromo-substituted BODIPY as synthons, while Hao et al. used bromo-substituted BODIPYs for regioselective substitution and Suzuki coupling reactions. Work by Arbeloa et al. demonstrated the selective functionalization of polyiodinated BODIPY precursors.<sup>[28]</sup> So far, three routes to obtaining halogenated BODIPY precursors for further functionalization have been established: 1) Total synthesis-type reactions via halogenations of the pyrrole ring, 2) halogenation of the dipyrromethane precursor, and 3) electrophilic aromatic substitution of the BODIPY framework. Heterocycle-fused [3,2-b] pyrrole-derived BODIPY features a long excitation wavelength, high extinction coefficient, high photostability as NIR chromophores, insensitivity to different solvent polarities as well as high brightness as a fluorophore.<sup>[29]</sup> Our earlier work demonstrated the use of thieno-fused BODIPYs as useful photosensitizers upon halogenation as they possessed a decent fluorescent potential.<sup>[30]</sup> Zhao et al. followed up with interesting work to develop non-symmetric thieno-fused BODIPYs as bright and tunable fluorescent dyes.<sup>[31]</sup> Recently, Shen et al. synthesized thieno-pyrroles as potential photosensitizers for PDT.<sup>[32]</sup> Overall, thieno-fused [3,2-b] pyrrole-derived BODIPYs show promise for functional use; therefore, versatile but robust synthetic approaches are needed to overcome the rigid synthetic protocol currently in practice with less varied synthetic outcomes. In addition, there are only few reports studying this class of BODIPYs as well as its behavior in vivo.

We report the synthesis of multi-functional NIR BODIPY agents based on the thieno-fused [3,2-b] pyrrole framework and their versatility as fluorophores for diagnostics, including small-animal non-invasive imaging and as photosensitizers, generating singlet oxygen via a novel thieno-pyrrole-fused BODIPY intermediate. The strategy to access the NIR agents involved 1) building a reactive BODIPY electrophile (**BDP635**) bearing bromo-substituents at the 2,8-positions with absorption in the visible region (635 nm) as an intermediate and 2) functionalizing the reactive BODIPY intermediate through transition-metal-catalyzed coupling and nucleophilic substitution reactions.

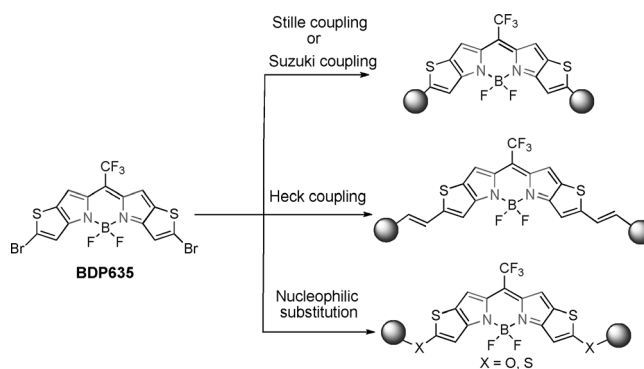
## Results and Discussion

### Synthesis

The essence of the strategy is that the red-emitting intermediate with halogen substitution at the 2,8-positions pro-

vides an excellent starting point and offers the use of mild reaction conditions to obtain NIR BODIPY agents, herein referred to as **SBDPIRs**, in moderate to high yield. The use of the thieno-pyrrole fusion creates flexibility in balancing the excited-state properties of these novel NIR BODIPY dyes.

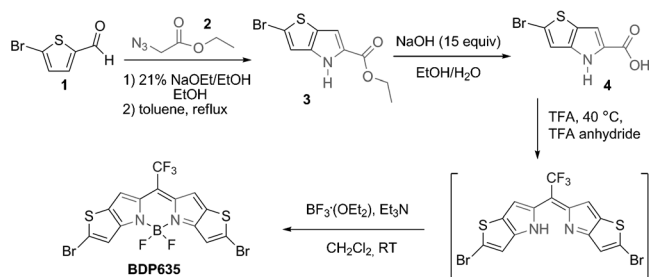
The rational design of the reactive thieno-pyrrole-fused BODIPY intermediate comprises a heteroaryl ring fusion of the traditional BODIPY core with thiophene, trifluoromethyl substitution at the *meso* position (as depicted in our previous work),<sup>[30]</sup> and an additional dibromo substitution positioned at the periphery of the core (Scheme 1). Compound



Scheme 1. Rational approach to the synthesis of rare multifunctional NIR BODIPY agents.

**4**, 2-bromo-4H-thieno[3,2-b]pyrrole-5-carboxylic acid, was obtained following the established Hemetsberger-Knittel synthesis using 5-bromo-2-thiophene carbaldehyde (**1**) and ethylazidoacetate (**2**) with subsequent hydrolysis (Scheme 2). The versatile BODIPY building block (**BDP635**) was then synthesized through a TFA-mediated condensation with TFA anhydride to obtain the CF<sub>3</sub> *meso*-substituted dipyrromethene unit (a proposed mechanism is presented in Scheme S1 and the ESI mass spectrum of decarboxylated acid **4** is given in Figure S3 in the Supporting Information) followed by boron difluoride chelation. Our next objective was to use this halide-substituted thieno-pyrrole-fused BODIPY (**BDP635**) as a platform to obtain NIR dyes, the **SBDPIRs**. The use of the Suzuki, Stille, and Heck coupling reactions with nucleophilic substitution reactions aided aryl functionalization (Scheme 3).

First, **BDP635** was subjected to Suzuki cross-coupling conditions for a relatively short reaction time of 2–3 hours



Scheme 2. Synthesis of the BODIPY intermediate **BDP635**.

with various aryl boronic acids (3–4 equiv) to afford diarylated SBDPIRs in 20–54% yield. The relatively short reaction time gives insight into the reactivity of **BDP635** in comparison to the reported hexabromo BODIPY.<sup>[24]</sup> The used boronic acids possessed different degrees of donor character from the dimethylphenyl, methoxyphenyl and trimethoxyphenyl to thiophenyl units and the functionalized hydroxyphenyl boronic acids. The Suzuki coupling reaction offered an opportunity to develop highly conjugated systems for the desired applications (Scheme 3). In addition, the functional group tolerance displayed by Suzuki reactions offers an additional advantage.

Second, we provide a useful alternative to the organoborane-based reactions by applying the Stille coupling using the organotin reagent tetraphenyltin. In this approach, the reaction was run for 1 hour to afford the diarylated **SBDPIr690** in 60% yield.

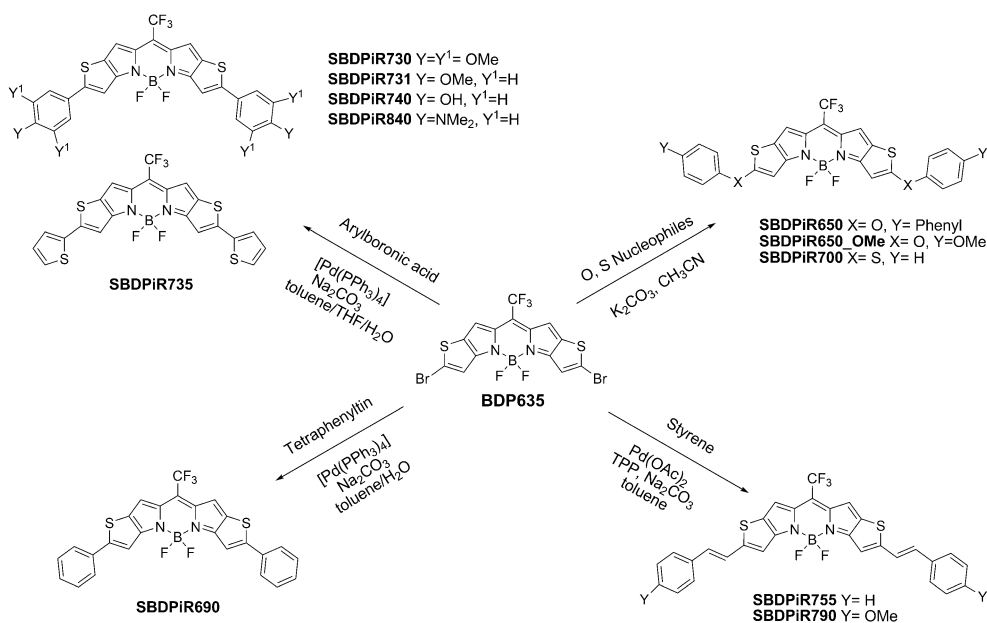
Third, we applied the Heck reaction to generate extended  $\pi$ -conjugated **SBDPIr**s in an attempt to induce a further redshift. The strategy involved connecting the aryl system to the BODIPY chromophore via an extended  $\pi$ -system. To demonstrate the reactivity of **BDP635** towards the Heck re-

action, styrene and the donor-effective 4-methoxystyrene were applied as reagents. Owing to the relatively high reactivity of **BDP635**, the reactions could be performed under less harsh conditions than those used with other BODIPY analogs.<sup>[31]</sup> This may be due to the fact that **BDP635** possesses a strong electron-withdrawing CF<sub>3</sub> group in addition to the halide substituents. We also used sodium bicarbonate as a base in this reaction instead of the commonly used triethylamine. The Heck reaction required a relatively longer reaction time (>6 h) among the **SBDPIr** series using about 3–6 equivalents of the vinyl substrates to afford the diarylated **SBDPIr755** and **SBDPIr790** in approximately 25% yield.

Finally, **BDP635** was reactive towards sulfur and oxygen nucleophiles, and the desired di-substituted products were formed within 0.5–1 h in yields of 25–70%. The reaction conditions to produce the ethers (**SBDPIr650** and **SBDPIr650\_Ome**) and thioether (**SBDPIr700**) were similar to those reported for the 3,5-dihalogenated BODIPY dyes.<sup>[34]</sup>

### X-ray Structure Analysis

Since the incorporation of heavy atoms with large atomic radii into chromophores may result in a deformation of the planar structure, we sought to gain insight into this structural effect, if any, on our versatile scaffold, **BDP635**, and indirectly on our new NIR BODIPY dyes, the **SBDPIr**s. To this end, **BDP635** was crystallized by the slow evaporation of its solution in dichloromethane at room temperature (Figure 2). The conjugated nature of the structure was confirmed by the comparable bond lengths for bridging (C6) to both pyrrole rings (C14, C15) of 1.397(3) Å and 1.406(4) Å, respectively, and by the comparable bond lengths of



Scheme 3. Palladium-catalyzed coupling and  $S_NAr$  reactions of **BDP635**.

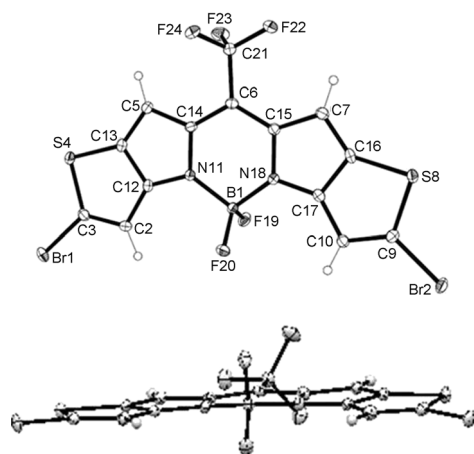


Figure 2. ORTEP view of the X-ray crystal structures of **BDP635**. Displacement ellipsoids are drawn at the 50% probability level.

1.545(4) Å and 1.549(4) Å, respectively, between the pyrrole nitrogen (N11, N18) and boron. Furthermore, the sterically crowded boron center maintained a geometry that was almost tetrahedral with an N-B-N angle of 105.1(2)° and an F-B-F angle of about 108.9(2)°. Despite the incorporation of the bromine atom, the angle of intersection of Br1 and Br2 to the thienopyrrole ring remained similar with C-C-Br angles of 125.7(2)° and 126.1(2)° respectively, thus indicating the preserved planarity of the central 18-atom core of **BDP635**.

### Theoretical Insights into the Intermediate

To understand the electronic and excited-state behaviors of **BDP635**, density functional theory (DFT) calculations were performed in vacuo. Geometry optimization was carried out using the 6-311G\* basis set, and the absorption-related excitation was calculated by using time-dependent DFT (TD-DFT), the CPCM model, and dichloromethane as solvent. The optimized structure also had a preserved planarity, as no significant change was found in the conformation (Figure 3). In addition, the frontier molecular orbital displayed an even electron distribution within the BODIPY chromophore in the HOMO and an electron pull effect in the LUMO by the trifluoromethyl group. The lack of donor groups influenced this HOMO-LUMO behavior and the energy gap of 2.02 eV, thus inducing a strong S<sub>0</sub>→S<sub>1</sub> transition in the visible region. The deviation between the predicted and the experimental absorption spectra was about 20 nm, thus demonstrating that DFT calculation is a useful tool for predicting UV/Vis spectra

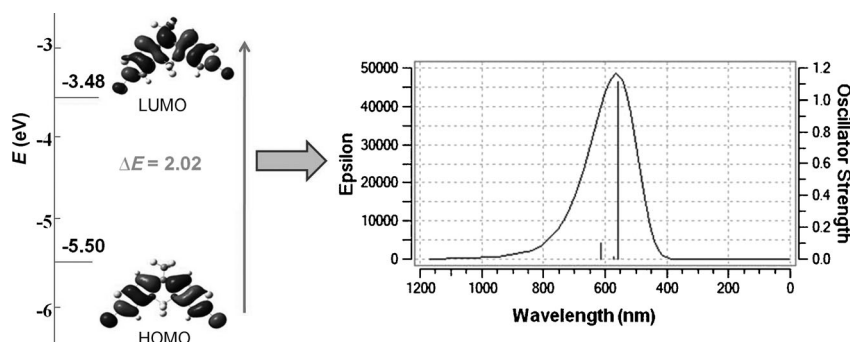


Figure 3. Quantum chemical calculations for **BDP635**.

of these dyes, taking into account solvent effects.

### Optical Properties

The spectroscopic characterization of the NIR BODIPY dyes was performed by studying their absorption and emission behavior in CHCl<sub>3</sub> (Figure 4). The absorption spectra of all **SBDPiRs** were comparable in shape to those of the previously reported boron dipyrromethene dyes, with the maximal absorption ascribed to the S<sub>0</sub>→S<sub>1</sub> transition and the ‘shoulder’ peak at a shorter wavelength assigned to the S<sub>0</sub>→S<sub>2</sub> transition. The **SBDPiRs** absorbed in a wide range of wavelengths (650–900 nm), presumably due to the combinational effects from the strengths of the π-electron donor and acceptor, extended π-conjugation, and effects of the sulfur atoms. Solutions of **SBDPiR650**, **SBDPiR650\_OMe**, and **SBDPiR700** in chloroform were blue and green, respectively. All three dyes exhibited fluorescence emission in the NIR region (660, 660, and 730 nm, respectively). **SBDPiR650** and **SBDPiR650\_OMe** absorbed at the shortest wavelengths in this series owing to the disruption of the π-conjugation by the O atom between the core and peripheral phenyl groups. On the other hand, **SBDPiR700** was less affected due to the effect imparted by the S atom. The impact of substituents at the phenyl groups on the spectral properties was clearly seen in **SBDPiR690**, **SBDPiR730**, **SBDPiR731**, **SBDPiR735**, **SBDPiR740**, and **SBDPiR840** (Table 1). These dyes displayed a vivid green to greenish brown color in organic solvents. The absorption shifted towards the red by about 40 nm from **SBDPiR690** when methoxyphenyl, trimethoxyphenyl, and hydroxyphenyl donor groups were used. The use of thiophene donor substituents is well known to impart significant red-shifting,<sup>[35]</sup> this was further confirmed in **SBDPiR735** by its absorption pattern. Interestingly, the use of dimethylaminophenyl moieties as donors induced an absorption >840 nm, a rare absorption observed for the BODIPY chromophore. We attribute the large bathochromic shift (>200 nm) from the starting **BDP635** to an internal charge transfer (ICT).<sup>[36]</sup> When the donor moieties were conjugated to the BODIPY chromophore via a vinylic bond, dark blue and greenish brown colors were observed for solutions of **SBDPiR755** and **SBDPiR790**, respectively. The extended π-conjugation by

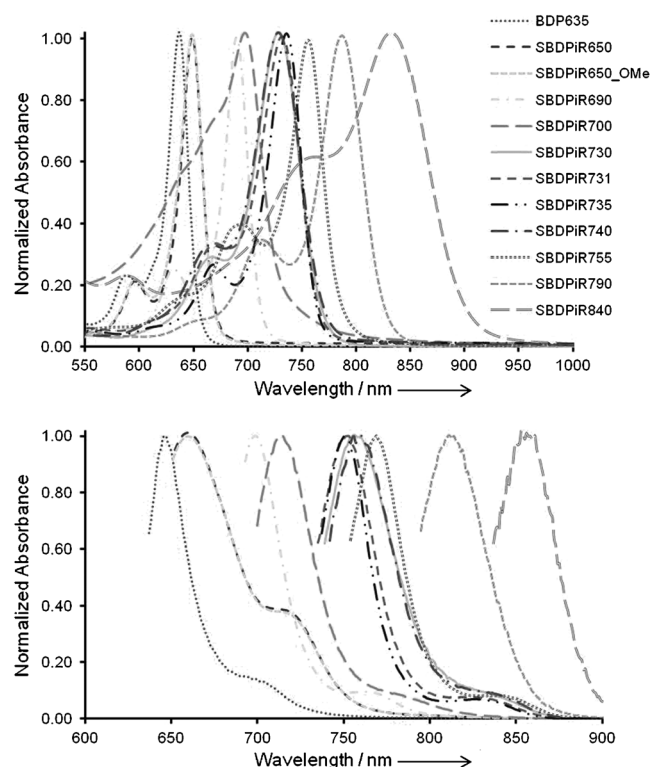


Figure 4. Absorption and emission spectra of **BDP635** and **SBDPIRs** in  $\text{CHCl}_3$  (**SBDPIR740** in EtOH).

separating the donor moieties from the BODIPY chromophore by a vinylic bond imparted a bathochromic shift of  $> 50$  nm (**SBDiR690**  $\rightarrow$  **SBDPIR755**; **SBDPIR731**  $\rightarrow$  **SBDPIR790**). The emission bands of the two dyes were in the NIR region of  $> 800$  nm.

### Singlet Oxygen Generation

We anticipated a degree of intersystem crossing (ISC) efficiency by these **SBDPIRs** due to the heavy-atom effect that may be potentially induced by the thieno fusion. The ISC efficiency was further supported by monitoring the capability of singlet oxygen ( $^1\text{O}_2$ ) generation by the photoexcited **SBDPIRs**, as detected by the phosphorescence spectra of  $^1\text{O}_2$  at 1270 nm (Figure 5). The highly reactive  $^1\text{O}_2$  is a cytotoxic species in PDT, which is generated by dyes called photosensitizers upon light illumination. The  $^1\text{O}_2$  generation efficiency ( $\Phi_\Delta$ ) decreased in the order of **BDP635**  $>$  **SBDPIR690**  $>$  **SBDPIR700**  $>$  **SBDPIR650**. The observation for **BDP635** was readily attributed to the additional bromo-substituents at the 2,8-positions. The capabilities of these agents to generate  $^1\text{O}_2$  coupled with their reasonable fluorescence emission ( $\Phi_F = 0.05, 0.22, 0.28,$  and  $0.86$ , respectively) suggest a possible application as NIR-active theranostic drugs for dual-functioning PDT and imaging.

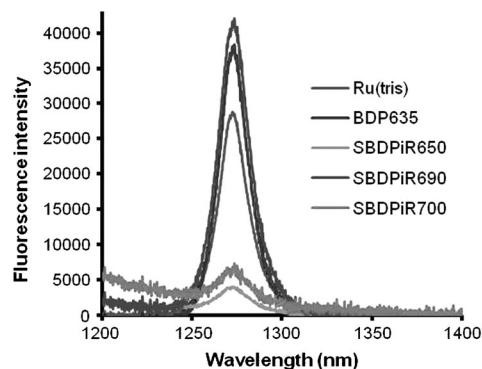


Figure 5. Phosphorescence spectra of singlet oxygen generated by **BDP635** and **SBDPIRs** in  $\text{CHCl}_3$ .

Table 1. Summary of the spectroscopic data.

Agent	$\lambda_{\text{max(abs)}}$ [nm]	$\lambda_{\text{max(flu)}}$ [nm]	$\epsilon^{[a]}$ [ $\text{M}^{-1} \text{cm}^{-1}$ ]	$\Phi_{\text{flu}}^{[b]}$	$\tau^{[c]}$ [ns]	$\Phi_\Delta^{[d]}$	$E_{1/2}$ (Ag/AgCl) <sup>[e]</sup>	
							Reduction	Oxidation
<b>BDP635</b>	635	650	150000	0.05	$< 0.1$	0.52	-0.18, -0.97	1.59
<b>SBDPIR650</b>	649	660	118000	0.86	4.14	0.02	-0.39, -1.07	1.16, 1.43, 1.99
<b>SBDPIR650_OMe</b>	649	660	121000	0.87	4.40	-	-0.56, -1.25	1.01, 1.42
<b>SBDPIR690</b>	688	700	120000	0.22	1.55	0.42	-0.93, -1.65	0.79, 1.04, 1.52
<b>SBDPIR700</b>	694	715	105000	0.28	3.28	0.05	-0.24, -0.86	0.97, 1.18
<b>SBDPIR730</b>	728	761	140000	0.23	2.60	-	-0.25, -0.92	1.17, 1.65
<b>SBDPIR731</b>	731	755	185000	0.38	3.22	-	-0.45, -1.13	0.98, 1.17, 1.36
<b>SBDPIR735</b>	733	763	125000	0.28	3.09	-	-0.35, -1.03	1.06
<b>SBDPIR740</b>	738	763	160000	0.10	1.20	-	-0.32	1.02, 1.26
<b>SBDPIR755</b>	753	785	110000	0.07	0.93	-	-0.23, -0.90	1.17, 1.5
<b>SBDPIR790</b>	786	810	85000	0.01	1.30	-	-0.26, -0.91	1.0, 1.16, 1.62
<b>SBDPIR840</b>	841	860	30000	0.002	0.90	-	-0.42	0.50

[a] Molar absorptivity measurements were carried out in  $\text{CHCl}_3$  except for **SBDPIR740** for which measurements were performed in EtOH. [b] The fluorescence quantum yield was determined in  $\text{CHCl}_3$  (MeOH for **SBDPIR740**) at 298 K with aza-BODIPY (**BDP635**–**SBDPIR700**) and **KFL4** (**SBDPIR730**–**SBDPIR840**) as reference ( $\Phi_{\text{flu}} = 0.34$  and  $0.56$  in  $\text{CHCl}_3$ , respectively). [c] Lifetimes are denoted as  $\tau$  for all agents. [d] Singlet oxygen quantum yields were determined in  $\text{CHCl}_3$  with  $[\text{Ru}(\text{bipy})_3]\text{Cl}_2$  as reference ( $\Phi_\Delta = 0.77$  in MeOH). [e] All potentials were determined from DPV plots of the agents.

### Electrochemistry

The electrochemical behaviors of all agents were also examined in  $\text{CH}_2\text{Cl}_2$  containing 0.1 M TBAP. Cyclic voltammograms are shown in Figure 6 and the redox potentials for each oxidation and reduction are listed in Table 1. The investigated compounds with the exception of **SBDPIR840** underwent two reversible reductions at  $E_{1/2} = -0.18$  to  $-0.93$  V and  $E_{1/2} = -0.66$  to  $-1.65$  V, to form the respective radical anion and dianion. Two-to-three oxidations were detected at  $E_{1/2} = 0.44$  to  $1.59$  V,  $E_{1/2} = 0.95$  to  $1.77$  V, and  $E_{1/2} = 1.36$  to  $1.99$  V,

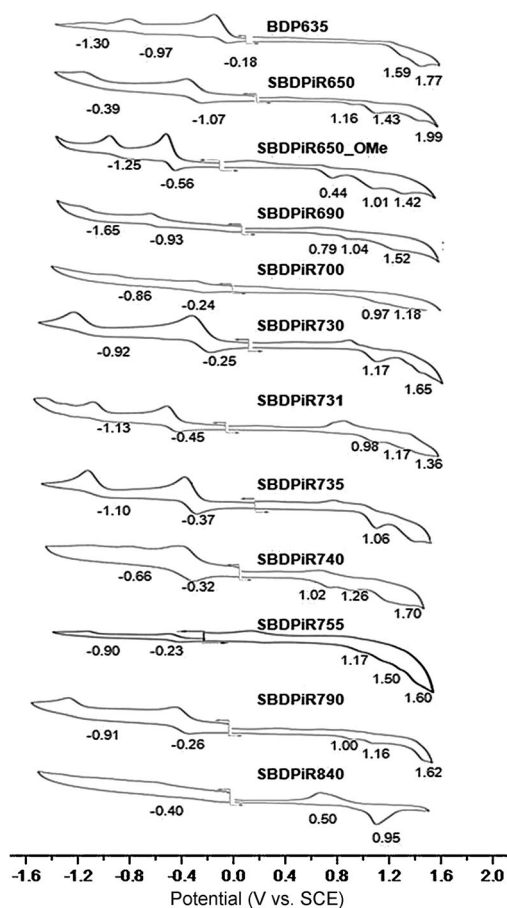


Figure 6. Cyclic voltammograms of **BDP635** and **SBDPIRs** in  $\text{CH}_2\text{Cl}_2$  containing 0.1 M TBAP at the scan rate of  $0.1 \text{ V s}^{-1}$ .

giving rise to dications and to trications, respectively. In addition, the first oxidation was largely reversible while the second and third oxidations were mostly quasi-reversible or irreversible, possibly because of the instability of the dication and trication generated. The multiple electrochemical waves might correspond to multiple electron transfers in the extensively conjugated BODIPY compounds, thus giving rise to radical anions and dianions on reduction and radical cations and dications on oxidation. The separation between oxidation waves, about 0.2–0.6 V, is within that of polycyclic aromatic compounds.<sup>[37]</sup> **BDP635** showed three reductive waves with a separation of 0.3 V between the second and third waves, possibly due to the instability of the dication generated. The HOMO–LUMO gap estimated from the first oxidation and first reduction potentials varied from 1.77 to 0.90 V, tracking the red-shift of the absorption and emission peak of the derivatives in Table 1.

### In Vivo Imaging

To demonstrate the use of these extraordinary NIR BODIPY dyes for in vivo fluorescence imaging, the time-dependent biodistribution of **SBDPIR740** in a living mouse was examined (Figure 7). This study, although not extensive, offers insight of the property of such fluorophores in biological tissue. **SBDPIR740** was selected due to its hydroxy groups that introduce a hydrophilic character to the lipophilic **SBDPIRs**, the availability of the phenolic groups for further modifications, and its compatibility with several imaging instruments with relative ease. A  $2.5 \mu\text{mol kg}^{-1}$  drug dose was injected into the intraperitoneal cavity of a female nude mouse. The mouse was imaged using an IVIS imaging system with excitation and emission filters set at 745 nm and 800 nm, respectively. In the first 10 min, **SBDPIR740** re-

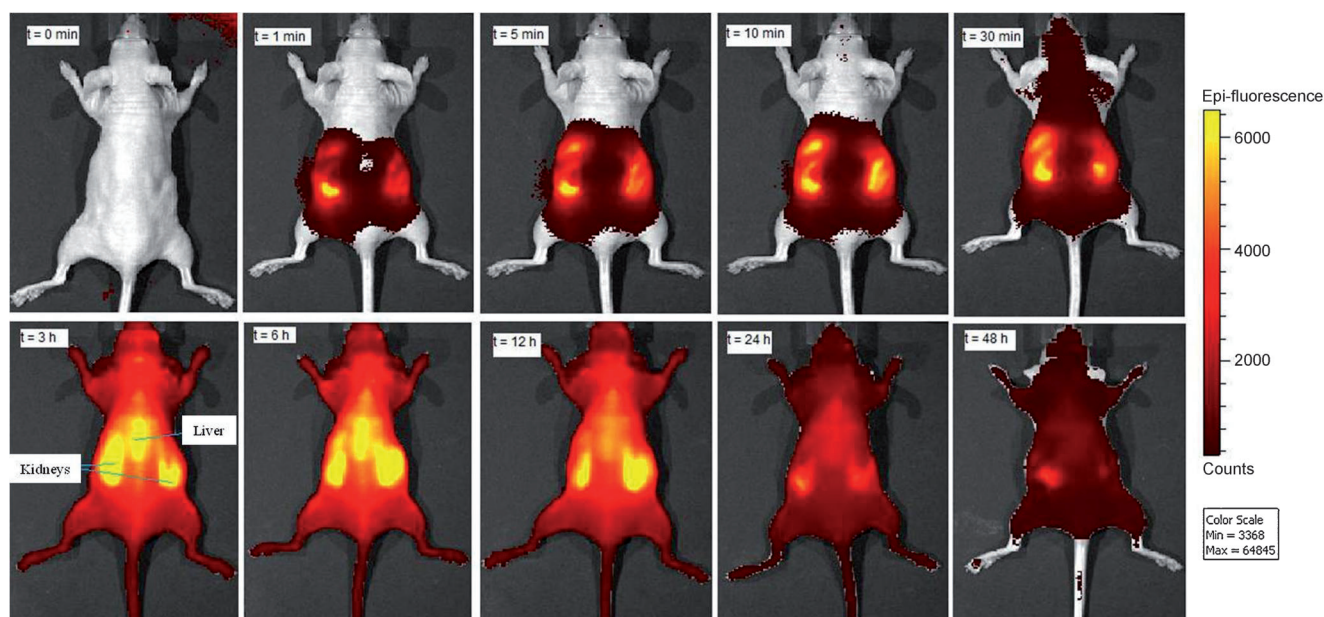


Figure 7. Mouse in vivo imaging with **SBDPIR740** ( $n=3$ ).

mained largely within the peritoneal cavity. At 30 min, it seemed that the dye had absorbed into the blood circulation, as fluorescence signals spread beyond the cavity towards the head region. Fluorescence intensities at the skin reached maximum levels between 3 h and 6 h. Kidneys and liver were observed as intense bright fluorescence spots. After 24 h, **SBDPIR740** was considerably cleared with a degree of fluorescence signal in the kidneys.

## Conclusions

In summary, the synthesis of a series of novel thieno-fused [3,2-*b*] pyrrole-derived NIR BODIPYs was achieved. Through a rational synthetic design of a versatile intermediate that possesses bromo-substituents at the 2,8-positions of the expanded BODIPY chromophore, palladium-catalyzed cross-coupling and nucleophilic substitution was readily accessible.

The spectroscopic data indicated that the incorporation of various donor moieties resulted in a rare bathochromic shift for BODIPYs, with absorbance maxima reaching 840 nm. The use of thiophene with low-lying excited states demonstrated an unprecedented singlet oxygen generation by these non-halogenated NIR BODIPYs. The non-halogenated SBDPIR photosensitizers have an added benefit of fluorescence emission, that is, they hold promise for fluorescence-guided PDT. Our study provides a useful electrochemical insight into these thieno-pyrrole-derived BODIPYs. The versatility of our approach is also demonstrated in the incorporation of functionalities for further conjugation to other materials, particularly, biomolecules for cellular and tissue targeting. We demonstrated the potential of the SBDPIRs for in vivo imaging using **SBDPIR740**. The time-dependent bio-distribution of this class of BODIPYs at a low dose ( $2.5 \mu\text{mol kg}^{-1}$ ) indicate that they may find use as dyes for in vivo imaging. Biological evaluation of these novel BODIPYs is currently under investigation and will be reported elsewhere. Further functionalization of these NIR dyes for specific biomedical applications in fluorescence optical imaging and PDT is in progress.

## Experimental Section

### General Methods

Chemical reagents and solvents of analytical grade were purchased from commercial suppliers (Sigma-Aldrich, USA; VWR, USA) and were used without purification. Air-sensitive reactions were performed under an atmosphere of nitrogen. NMR spectra were recorded in  $\text{CDCl}_3$ ,  $\text{CD}_2\text{Cl}_2$ ,  $[\text{D}_6]\text{acetone}$ , or  $[\text{D}_6]\text{DMSO}$  by using a Varian 300 MHz spectrometer. Chemical shifts are given in parts per million relative to TMS or 7.23 ppm for residual  $\text{CHCl}_3$ . Coupling constants were measured in Hz. High-resolution mass spectrometry measurements were performed using electron impact at an ionized voltage of 70 eV and electrospray (ESI) ionization mass spectrometry was done with a QTOF-1 analyzer.

### Theoretical Calculations

Geometry optimization was performed with Gaussian 09<sup>[38]</sup> using density functional theory (DFT). Electronic excitation was computed using the time-dependent (TD)-DFT calculation at the B3LYP/PBE PBE<sup>[39]</sup> level using the CPCM model in dichloromethane as solvent.

### 2-Bromo-4*H*-thieno [3, 2-*b*] pyrrole-5-carboxylic acid (**4**)

Compound **3** (0.30 g, 1.1 mmol) was dissolved in EtOH (10 mL). Subsequently, NaOH (0.62 g, 15.5 mmol) in water (5 mL) was added, and the mixture was refluxed for 1 h. The reaction was then cooled to room temperature and chilled in an ice bath to acidify the mixture with concentrated HCl. The precipitate was filtered, washed with water, and dried under vacuum to afford **4** as a gray solid (0.22 mg, 70%). <sup>1</sup>H NMR ( $[\text{D}_6]\text{DMSO}$ , 300 MHz):  $\delta = 12.76$  (s, 1H), 12.15 (s, 1H), 7.21 (s, 1H), 6.99 ppm (s, 1H); HRMS ESI ( $m/z$ ): calcd for  $\text{C}_7\text{H}_4\text{BrNO}_2\text{S}$ : 246.0812; found: 245.9224  $[\text{M}+\text{H}]^+$ . We should note that **4** has been previously reported and was prepared by the published method with slight modifications.<sup>[28]</sup>

### 2,8-Di(bromo)-11-trifluoromethyl-dithieno[2,3-*b*]-[3,2*g*]-5,5-difluoro-5-bora-3*a*,4*a*-dithio-s-indacene (**BDP635**)

Compound **4** (1.0 g, 1.8 mmol) was dissolved in TFA (25 mL) and heated to 40 °C for 15 min, upon an intense red color appeared. Subsequently, trifluoroacetic anhydride (9 mL) was added and the temperature was then raised to 80 °C with continued stirring for 4 h. The resulting deep blue reaction solution was then allowed to cool to room temperature and poured into an aqueous  $\text{NaHCO}_3$  solution containing crushed ice. The resultant precipitate was then filtered and dried in vacuo. The dry solid was then dissolved in  $\text{CH}_2\text{Cl}_2$  (250 mL) and stirred for 5 min at room temperature under a nitrogen atmosphere. Next, boron trifluoride dietherate (4 mL) and triethylamine (3 mL) were added and the reaction mixture was stirred at room temperature for 1 h. Following evaporation of the solvent, the crude product was purified by flash chromatography on silica gel ( $\text{CH}_2\text{Cl}_2$ ) to afford **BDP635** as a bluish-green metallic solid (160 mg, 16%). <sup>1</sup>H NMR ( $\text{CDCl}_3$ , 300 MHz):  $\delta = 7.31$  (s, 2H), 7.24 ppm (s, 2H); <sup>13</sup>C NMR:  $\delta = 159.4$ , 137.5, 136.0, 131.5, 119.3, 117.2, 114.6, 112.0 ppm; HRMS EI ( $m/z$ ): calcd for  $\text{C}_{14}\text{H}_4\text{BBr}_2\text{F}_3\text{N}_2\text{S}_2$ : 529.8200; found: 529.8170  $[\text{M}]^+$ .

### 2,8-Di(4-hydroxyphenyl)-11-trifluoromethyl-dithieno[2,3-*b*]-[3,2*g*]-5,5-difluoro-5-bora-3*a*,4*a*-diazas-indacene (**SBDPIR740**)

To a solution of **BDP635** (0.19 g, 0.36 mmol) in toluene/THF/ $\text{H}_2\text{O}$  (30 mL, 1:1:1) was added 4-hydroxyboronic acid (0.20 g, 1.43 mmol) and  $\text{Na}_2\text{CO}_3$  (0.11 g 1.05 mmol). The reaction solution was purged by bubbling nitrogen gas through for 10 min. A catalytic amount of  $[\text{Pd}(\text{PPh}_3)_4]$  (22 mg, ~5 mol%) was added and the reaction was heated to 80 °C for 2 h. After completion of the reaction as judged by TLC, the reaction was diluted with 5 mL water and extracted with diethyl ether. The combined organic layer was washed with water and brine (100 mL each), respectively, and dried over anhydrous  $\text{Na}_2\text{SO}_4$ . The dried mixture was purified by silica-gel column chromatography (EtOAc/*n*-hexane 1:1) to afford **SBDPIR740** as a dark green solid (102 mg, 54%, purity: 99.3% based on HPLC, see Figure S7 in the Supporting Information). <sup>1</sup>H NMR ( $[\text{D}_6]\text{acetone}$ , 300 MHz):  $\delta = 7.84$  (d,  $J = 9.0$  Hz, 4H), 7.52 (s, 2H), 7.37 (s, 2H) 7.03 ppm (d,  $J = 9.0$  Hz, 4H); <sup>13</sup>C NMR:  $\delta = 150.3$ , 134.4, 131.7, 130.2, 129.2, 128.4, 119.3, 115.9, 115.6, 115.1 ppm; HRMS EI ( $m/z$ ): calcd for  $\text{C}_{26}\text{H}_{14}\text{BF}_3\text{N}_2\text{O}_2\text{S}_2$ : 556.0510; found: 556.0520  $[\text{M}]^+$ .

### 2,8-Di(4-methoxyphenyl)-11-trifluoromethyl-dithieno[2,3-*b*]-[3,2*g*]-5,5-difluoro-5-bora-3*a*,4*a*-diazas-indacene (**SBDPIR731**)

The method described for **SBDPIR740** was followed using **BDP635** (0.10 g, 0.2 mmol), 4-methoxyphenylboronic acid (0.12 g, 0.8 mmol), and  $\text{Na}_2\text{CO}_3$  (0.06 g 0.6 mmol). The dried mixture was purified by silica-gel column chromatography (EtOAc/toluene 5:95) to afford **SBDPIR731** as a dark green solid (53 mg, 50%). <sup>1</sup>H NMR ( $\text{CD}_2\text{Cl}_2$ , 400 MHz):  $\delta = 7.76$  (d,  $J = 8.0$  Hz, 4H), 7.34 (s, 2H), 7.32 (s, 2H), 7.03 (d,  $J = 8.0$  Hz, 4H), 3.91 ppm (s, 6H); HRMS EI ( $m/z$ ): calcd for  $\text{C}_{28}\text{H}_{18}\text{BF}_3\text{N}_2\text{O}_2\text{S}_2$ : 584.0823; found: 584.0825  $[\text{M}]^+$ .

*2,8-Di(thiophenyl)-11-trifluoromethyl-dithieno[2,3-b]-[3,2g]-5,5-difluoro-5-bora-3a,4a-diaza-s-indacene (SBDPIR735)*

The method described for **SBDPIR740** was followed using **BDP635** (0.10 g, 0.2 mmol), 2-thiopheneboronic acid (0.10 g, 0.8 mmol), and  $\text{Na}_2\text{CO}_3$  (0.06 g 0.6 mmol). The dried mixture was purified by silica-gel column chromatography (EtOAc/toluene 5:95) to afford **SBDPIR735** as a dark green solid (51 mg, 50%).  $^1\text{H NMR}$  ( $\text{CD}_2\text{Cl}_2$ , 300 MHz):  $\delta = 7.24$  (m, 2H), 7.53 (s, 2H), 7.54 (s, 2H), 7.34 (s, 2H), 7.57 ppm (m, 4H);  $^{13}\text{C NMR}$ :  $\delta = 134.6$ , 134.3, 130.8, 130.5, 129.6, 128.7, 128.1, 128.0, 127.9, 118.2, 108.6 ppm; HRMS EI ( $m/z$ ): calcd for  $\text{C}_{22}\text{H}_{10}\text{BF}_3\text{N}_2\text{S}_4$ : 535.9740; found: 535.9725 [ $M$ ] $^+$ .

*2,8-Di(3,4,5-trimethoxyphenyl)-11-trifluoromethyl-dithieno[2,3-b]-[3,2g]-5,5-difluoro-5-bora-3a,4a-diaza-s-indacene (SBDPIR730)*

The method described for **SBDPIR740** was followed using **BDP635** (0.12 g, 0.2 mmol), 3,4,5-trimethoxyphenylboronic acid (0.19 g, 0.9 mmol), and  $\text{Na}_2\text{CO}_3$  (0.07 g 0.7 mmol). The reaction solution was purged by bubbling nitrogen gas through for 10 min. The dried mixture was purified by silica-gel column chromatography (EtOAc/toluene 5:95) to afford **SBDPIR730** as a dark green solid (54 mg, 45%).  $^1\text{H NMR}$  ( $\text{CD}_2\text{Cl}_2$ , 300 MHz):  $\delta = 7.36$  (s, 2H), 7.32 (s, 2H), 6.98 (s, 4H), 3.93 (s, 12H), 3.87 ppm (s, 6H);  $^{13}\text{C NMR}$ :  $\delta = 163.0$ , 160.9, 153.7, 140.9, 138.4, 134.3, 129.1, 118.4, 108.5, 104.2, 60.7, 56.2 ppm; HRMS EI ( $m/z$ ): calcd for  $\text{C}_{32}\text{H}_{26}\text{BF}_3\text{N}_2\text{O}_6\text{S}_2$ : 704.1245, found: 704.1226 [ $M$ ] $^+$ .

*2,8-Di(4-N,N-dimethylaminophenyl)-11-trifluoromethyl-dithieno[2,3-b]-[3,2g]-5,5-difluoro-5-bora-3a,4a-diaza-s-indacene (SBDPIR840)*

The method described for **SBDPIR740** was followed using **BDP635** (0.12 g, 0.2 mmol), 4-N,N-dimethylaminophenylboronic acid (0.11 g, 0.7 mmol), and  $\text{Na}_2\text{CO}_3$  (0.07 g 0.7 mmol). The dried mixture was purified by silica-gel column chromatography (toluene) to afford **SBDPIR840** as a dark green solid (24 mg, 20%).  $^1\text{H NMR}$  ( $\text{CD}_2\text{Cl}_2$ , 300 MHz):  $\delta = 8.15$  (d,  $J = 6.0$  Hz, 4H), 7.70–7.50 (m, 3H), 6.70 (s, 1H), 6.85 (d,  $J = 6.0$  Hz, 4H), 2.95 (s, 12H);  $^{13}\text{C NMR}$ :  $\delta = 153.4$ , 136.8, 136.3, 136.0, 134.0, 131.9, 130.0, 128.5, 126.9, 116.4, 112.4, 111.0, 40.3, 39.8 ppm; HRMS EI ( $m/z$ ): calcd for  $\text{C}_{30}\text{H}_{24}\text{BF}_3\text{N}_4\text{S}_2$ : 610.1456, found: 610.1470 [ $M$ ] $^+$ .

*2,8-Di(styryl)-11-trifluoromethyl-dithieno[2,3-b]-[3,2g]-5,5-difluoro-5-bora-3 a,4 a-diaza-s-indacene (SBDPIR755)*

**BDP635** (0.08 g, 0.2 mmol), styrene (0.04 g, 0.4 mmol),  $\text{Pd}(\text{OAc})_2$  (20 mol%), triphenylphosphine (20 mol%), and  $\text{Na}_2\text{CO}_3$  (0.06 g 0.6 mmol) were dissolved in anhydrous toluene (3 mL). The reaction mixture was then heated to 80°C with stirring under nitrogen for 6 h. After completion (monitored by TLC), the mixture was diluted with 10 mL toluene, washed with water and brine (50 mL each), and dried over anhydrous  $\text{Na}_2\text{SO}_4$ . The dried mixture was purified by silica-gel column chromatography (toluene) to afford **SBDPIR755** as a black solid (17 mg, 22%).  $^1\text{H NMR}$  ( $\text{CD}_2\text{Cl}_2$ , 300 MHz):  $\delta = 7.59$  (d,  $J = 8.0$  Hz, 4H), 7.39 (d,  $J = 8.0$  Hz, 4H), 7.26 (s, 3H), 7.20 (s, 1H), 7.12 ppm (s, 2H);  $^{13}\text{C NMR}$ :  $\delta = 161.3$ , 158.9, 135.6, 129.6, 128.9, 127.3, 122.9, 111.8 ppm; HRMS EI ( $m/z$ ): calcd for  $\text{C}_{30}\text{H}_{18}\text{BF}_3\text{N}_2\text{S}_2$ : 576.0925; found: 576.0906 [ $M$ ] $^+$ .

*2,8-Di(4(methoxy-phenyl)vinyl)-11-trifluoromethyl-dithieno[2,3-b]-[3,2g]-5,5-difluoro-5-bora-3a,4a-diaza-s-indacene (SBDPIR790)*

The method described for **SBDPIR755** was followed using **BDP635** (0.08 g, 0.2 mmol), 4-methoxystyrene (0.04 g, 0.4 mmol),  $\text{Pd}(\text{OAc})_2$  (20 mol%), triphenylphosphine (20 mol%), and  $\text{Na}_2\text{CO}_3$  (0.06 g 0.6 mmol) dissolved in anhydrous toluene (3 mL). The dried mixture was purified by silica-gel column chromatography (toluene) to afford **SBDPIR790** as a dark brown solid (20 mg, 25%).  $^1\text{H NMR}$  ( $\text{CD}_2\text{Cl}_2$ , 300 MHz):  $\delta = 7.44$  (d,  $J = 9.0$  Hz, 4H), 7.17 (s, 2H), 7.16 (s, 2H), 7.15 (s, 2H), 6.99 (s, 2H), 6.88 ppm (d,  $J = 9.0$  Hz, 4H);  $^{13}\text{C NMR}$ :  $\delta = 161.5$ , 135.2, 134.9, 134.3, 129.0, 128.7, 128.1, 127.3, 120.6, 117.2, 114.6, 114.1, 113.6, 111.3, 55.4 ppm; HRMS EI ( $m/z$ ): calcd for  $\text{C}_{32}\text{H}_{22}\text{BF}_3\text{N}_2\text{O}_2\text{S}_2$ : 636.1136; found: 636.1120 [ $M$ ] $^+$ .

*2,8-Di(phenyl)-11-trifluoromethyl-dithieno[2,3-b]-[3,2g]-5,5-difluoro-5-bora-3 a,4 a-diaza-s-indacene (SBDPIR690)*

**BDP635** (0.03 g, 0.1 mmol), tetraphenyltin (0.03 g, 0.1 mmol),  $[\text{Pd}(\text{PPh}_3)_4]$  (20 mol%), triphenylphosphine (20 mol%), and  $\text{Na}_2\text{CO}_3$  (2 mL, 1 M aq.) were dissolved in toluene (3 mL). The reaction solution was heated to 80°C with stirring under nitrogen for 1 h. After completion (monitored by TLC), the reaction was diluted with 10 mL toluene, washed with water and brine (50 mL each) and dried over anhydrous  $\text{Na}_2\text{SO}_4$ . The dried mixture was purified by silica-gel column chromatography (toluene) to afford as **SBDPIR690** as a green solid (10 mg, 60%).  $^1\text{H NMR}$  ( $\text{CD}_2\text{Cl}_2$ , 300 MHz):  $\delta = 7.80$  (s, 1H), 7.70 (s, 1H), 7.60 (d,  $J = 8.0$  Hz, 4H), 7.50 (s, 1H), 7.41 ppm (peaks overlap, 7H);  $^{13}\text{C NMR}$ :  $\delta = 163.3$ , 161.3, 137.9, 137.3, 137.1, 136.9, 130.7, 129.8, 129.2, 128.9, 128.6, 128.2, 126.7 ppm; HRMS EI ( $m/z$ ): calcd for  $\text{C}_{26}\text{H}_{14}\text{BF}_3\text{N}_2\text{S}_2$ : 524.0612; found: 524.0599 [ $M$ ] $^+$ .

*2,8-Di(thiophenoxy)-11-trifluoromethyl-dithieno[2,3-b]-[3,2g]-5,5-difluoro-5-bora-3a,4a-diaza-s-indacene (SBDPIR700)*

**BDP635** (0.03 g, 0.06 mmol), thiophenol (0.02 g, 0.14 mmol), and  $\text{K}_2\text{CO}_3$  (0.02 g, 0.14 mmol) were dissolved in anhydrous  $\text{CH}_3\text{CN}$  (3 mL). The reaction solution was heated to 80 °C with stirring under nitrogen for 30 min, upon which the reaction turned red. After completion (monitored by TLC), the mixture was diluted with 10 mL  $\text{Et}_2\text{O}$ , washed with 1 M  $\text{Na}_2\text{CO}_3$  (aq.) (50 mL) and dried over anhydrous  $\text{Na}_2\text{SO}_4$ . The dried mixture was purified by silica-gel column chromatography (toluene) to afford **SBDPIR700** as a green solid (10 mg, 30%).  $^1\text{H NMR}$  ( $\text{CD}_2\text{Cl}_2$ , 300 MHz):  $\delta = 7.62$  (d,  $J = 6.0$  Hz, 4H), 7.47 (d,  $J = 6.0$  Hz, 4H), 7.24 (s, 2H), 7.15 (s, 2H), 6.91 ppm (s, 2H);  $^{13}\text{C NMR}$ :  $\delta = 161.9$ , 159.6, 134.7, 133.5, 133.9, 133.0, 132.9, 131.1, 129.9, 129.8, 129.7, 129.6, 117.6, 111.8, 113.3 ppm; HRMS EI ( $m/z$ ): calcd for  $\text{C}_{26}\text{H}_{14}\text{BF}_3\text{N}_2\text{S}_4$ : 588.0053; found: 588.0037 [ $M$ ] $^+$ .

*2,8-Di(4-methoxyphenoxy)-11-trifluoromethyl-dithieno[2,3-b]-[3,2g]-5,5-difluoro-5-bora-3a,4a-diaza-s-indacene (SBDPIR650\_OME)*

**BDP635** (0.06 g, 0.1 mmol), 4-methoxyphenol (0.06 g, 0.3 mmol), and  $\text{K}_2\text{CO}_3$  (0.05 g, 0.4 mmol) were dissolved in anhydrous  $\text{CH}_3\text{CN}$  (3 mL). The reaction mixture was then heated to 80°C with stirring under nitrogen for 30 min. After completion of the reaction (monitored by TLC), the mixture was dried, dissolved in  $\text{CH}_2\text{Cl}_2$ , washed with water and brine (50 mL each) and dried over anhydrous  $\text{Na}_2\text{SO}_4$ . The dried mixture was purified by silica-gel column chromatography (*n*-hexane) to afford **SBDPIR650\_OME** as a blue solid (15 mg, 25%).  $^1\text{H NMR}$  ( $\text{CD}_2\text{Cl}_2$ , 300 MHz):  $\delta = 7.22$  (d,  $J = 8.0$  Hz, 4H) 7.20 (s, 2H), 6.90 (d,  $J = 8.0$  Hz, 4H), 6.21 (s, 2H), 3.77 ppm (s, 6H);  $^{13}\text{C NMR}$ :  $\delta = 179.3$ , 158.1, 157.7, 149.3, 135.0, 125.7, 121.1, 118.6, 114.8, 94.9, 55.6 ppm; HRMS EI ( $m/z$ ): calcd for  $\text{C}_{28}\text{H}_{18}\text{BF}_3\text{N}_2\text{O}_4\text{S}_2$ : 616.0721; found: 616.0724 [ $M$ ] $^+$ .

*2,8-Di(biphenyl-4-yloxy)-11-trifluoromethyl-dithieno[2,3-b]-[3,2g]-5,5-difluoro-5-bora-3a,4a-diaza-s-indacene (SBDPIR650)*

**BDP635** (0.06 g, 0.1 mmol), 4-phenylphenol (0.06 g, 0.3 mmol), and  $\text{K}_2\text{CO}_3$  (0.05 g, 0.4 mmol) were dissolved in anhydrous  $\text{CH}_3\text{CN}$  (3 mL). The reaction mixture was then heated to 80°C with stirring under nitrogen for 30 min. After completion of the reaction (monitored by TLC), the mixture was diluted with 10 mL toluene, washed with water and brine (50 mL each) and dried over anhydrous  $\text{Na}_2\text{SO}_4$ . The dried mixture was purified by silica-gel column chromatography (EtOAc/*n*-hexane 1:1) to afford **SBDPIR650** as a reddish-brown solid (42 mg, 70%).  $^1\text{H NMR}$  ( $\text{CDCl}_3$ , 300 MHz):  $\delta = 7.52$  (m, 3H), 7.49 (m, 5H) 7.43 (m, 5H), 7.30 (d,  $J = 9.0$  Hz, 3H), 7.20 (s, 1H), 6.80 (d,  $J = 9.0$  Hz, 2H), 6.39 ppm (s, 1H);  $^{13}\text{C NMR}$ :  $\delta = 178.0$ , 157.7, 155.0, 139.7, 133.7, 128.8, 128.6, 128.2, 127.6, 126.9, 126.6, 126.5, 121.3, 120.1, 118.6, 115.5, 95.9 ppm; HRMS EI ( $m/z$ ): calcd for  $\text{C}_{38}\text{H}_{22}\text{BF}_3\text{N}_2\text{O}_2\text{S}_2$ : 708.1136; found: 708.1121 [ $M$ ] $^+$ .

*Electrochemical Measurements*

Cyclic voltammetry was performed with a homemade three-electrode cell that consisted of a platinum button or glassy carbon working electrode, a platinum wire counter-electrode, and a saturated calomel reference electrode (SCE). The SCE was separated from the bulk of the solution

by a fritted-glass bridge of low porosity which contained the solvent/supporting electrolyte mixture (tetra-*n*-butylammonium perchlorate, TBAP in *o*-DCB).

#### Photophysical Measurements

Absorption spectra were recorded on a Perkin Elmer lambda 25 UV/Vis spectrometer. Steady-state and lifetime fluorescence were measured using a Horiba Jobin Yvon UV/Vis/NIR fluorimeter attached with a Data Station v2.4 equipped with a Horiba NanoLED. Relative fluorescence quantum yields ( $\Phi_F$ ) were estimated using **KFL4** in chloroform ( $\Phi_F=0.56$ ) as a reference. Fluorescence lifetimes were determined by a single exponential curve fit. Singlet oxygen luminescence spectra at 1270 nm were recorded by using Horiba Jobin Yvon UV-Vis/NIR fluorimeter equipped with a FluorEssence v3.5 system. To measure the extinction coefficient, an SBDPIR (ca. 1 mg) was dissolved in chloroform (50 mL), and serially diluted to yield different dye concentrations ( $10^{-7}$ – $10^{-6}$  M) from the stock solution. A graph of the absorbance (A) versus concentration (C) was plotted and the extinction coefficient was determined by using the Lambert–Beer law. The fluorescence emission spectra of **SBDPIRs** using **KFL4** and **aza-BODIPY** as reference standards were recorded at 25°C. Dilute solutions of all dyes were prepared to compare their fluorescence emission spectra after excitation at 710 nm. The quantum yields were calculated following standard protocols.<sup>[9,40]</sup> Five serial dilutions were made with chloroform as a solvent, and the absorbance (A) of these solutions was less than 0.1. The integrated fluorescence intensity (F) at each concentration was recorded after excitation at 710 nm. A graph of F versus A was plotted to generate the gradient (G). The quantum yield was calculated using the equation:

$$\Phi_x = \Phi_{\text{std}} \left( \frac{G_x}{G_{\text{std}}} \right) \left( \frac{\eta_x^2}{\eta_{\text{std}}^2} \right)$$

Where the subscripts std and x denote the standard and test sample respectively,  $\Phi$  is the fluorescence quantum yield,  $G$  is the gradient from the plot of integrated fluorescence intensity vs. absorbance, and  $\eta$  is the refractive index of the solvent. The quantum yield of **KFL4** was 0.56 in chloroform.

#### In Vivo Optical Imaging

Optical imaging was performed with an IVIS Spectrum small-animal in vivo imaging system. The Living Image Software v3.0 was used to analyze images and measurements of fluorescent signals. Excitation and emission wavelengths of 745 nm and 800 nm, respectively, were used to acquire in-vivo fluorescent images of **SBDPIR740** ( $MW=556.05 \text{ g mol}^{-1}$ ). All images were attained using a 0.5 s exposure time and an  $f/\text{stop}$  of 1, with a sampling of multiple angles with the animal under Isoflurane anaesthesia. Animals were injected with  $2.5 \mu\text{mol kg}^{-1}$  of **SBDPIR740** via i.p. administration. The injection solution was prepared by solubilizing **SBDPIR740** in ethanol (4 mM) followed by dilution with PBS containing 1% Tween 80 and 5% dextrose. The solution was filtered through a 0.2  $\mu\text{m}$  sterile syringe filter before i.p. injection.

## Acknowledgements

The work was funded by OCAST (HR11-58). The authors thank the NSF (grant CHE-0130835 to YY and CHE-1110942 to FD) and the University of Oklahoma for funds to purchase the X-ray instrument and computers. The **BDP635** structure was determined by Douglas R. Powell at the Chemical Crystallography Laboratory at the University of Oklahoma. We thank the Peggy and Charles Stephenson Cancer Center at the University of Oklahoma, Oklahoma City, OK and an Institutional Development Award (IDeA) from the National Institute of General Medical Sciences of the National Institutes of Health under grant number P20 GM103639 for the use of the Molecular Imaging Core, which provided optical in vivo imaging service.

- [1] G. Qian, Z. Y. Wang, *Chem. Asian J.* **2010**, *5*, 1006–1029.
- [2] A. Yuan, J. Wu, X. Tang, L. Zhao, F. Xu, Y. Hu, *J. Pharm. Sci.* **2013**, *102*, 6–28.
- [3] K. Y. Law, *Chem. Rev.* **1993**, *93*, 449–486.
- [4] S. A. Hilderbrand, R. Weissleder, *Curr. Opin. Chem. Biol.* **2010**, *14*, 71–79.
- [5] M. Ethirajan, Y. H. Chen, P. Joshi, R. K. Pandey, *Chem. Soc. Rev.* **2011**, *40*, 340–362.
- [6] J. O. Escobedo, O. Rusin, S. Lim, R. M. Strongin, *Curr. Opin. Chem. Biol.* **2010**, *14*, 64–70.
- [7] A. Loudet, K. Burgess, *Chem. Rev.* **2007**, *107*, 4891–4932.
- [8] G. Ulrich, R. Ziessel, A. Harriman, *Angew. Chem.* **2008**, *120*, 1202–1219; *Angew. Chem. Int. Ed.* **2008**, *47*, 1184–1201.
- [9] K. Umezawa, Y. Nakamura, H. Makino, D. Citterio, K. Suzuki, *J. Am. Chem. Soc. J. Am. Chem. Soc.* **2008**, *130*, 1550.
- [10] S. G. Awuah, Y. You, *RSC Adv.* **2012**, *2*, 11169–11183.
- [11] A. Kamkaew, S. H. Lim, H. B. Lee, L. V. Kiew, L. Y. Chung, K. Burgess, *Chem. Soc. Rev.* **2013**, *42*, 77–88.
- [12] T. Bura, P. Retailleau, R. Ziessel, *Angew. Chem.* **2010**, *122*, 6809–6813; *Angew. Chem. Int. Ed.* **2010**, *49*, 6659–6663.
- [13] N. Boens, V. Leen, W. Dehaen, *Chem. Soc. Rev.* **2012**, *41*, 1130–1172.
- [14] V. V. Roznyatovskiy, C. H. Lee, J. L. Sessler, *Chem. Soc. Rev.* **2013**, *42*, 1921–1933.
- [15] M. Baruah, W. W. Qin, N. Basaric, W. M. De Borggraeve, N. Boens, *J. Org. Chem.* **2005**, *70*, 4152–4157.
- [16] M. Baruah, W. W. Qin, R. A. L. Vallee, D. Beljonne, T. Rohand, W. Dehaen, N. Boens, *Org. Lett.* **2005**, *7*, 4377–4380.
- [17] V. Leen, P. Yuan, L. Wang, N. Boens, W. Dehaen, *Org. Lett.* **2012**, *14*, 6150–6153.
- [18] J. Y. Han, O. Gonzalez, A. Aguilar-Aguilar, E. Pena-Cabrera, K. Burgess, *Org. Biomol. Chem.* **2009**, *7*, 34–36.
- [19] M. R. Rao, S. M. Mobin, M. Ravikanth, *Tetrahedron* **2010**, *66*, 1728–1734.
- [20] V. Leen, T. Leemans, N. Boens, W. Dehaen, *Eur. J. Org. Chem.* **2011**, 4386–4396.
- [21] V. Leen, D. Miscoria, S. C. Yin, A. Filarowski, J. M. Ngongo, M. Van der Auwerer, N. Boens, W. Dehaen, *J. Org. Chem.* **2011**, *76*, 8168–8176.
- [22] L. J. Jiao, J. L. Li, S. Z. Zhang, C. Wei, E. H. Hao, M. G. H. Vicente, *New J. Chem.* **2009**, *33*, 1888–1893.
- [23] L. J. Jiao, C. J. Yu, T. Uppal, M. M. Liu, Y. Li, Y. Y. Zhou, E. H. Hao, X. K. Hu, M. G. H. Vicente, *Org. Biomol. Chem.* **2010**, *8*, 2517–2519.
- [24] L. J. Jiao, C. J. Yu, M. M. Liu, Y. C. Wu, K. B. Cong, T. Meng, Y. Wang, E. H. Hao, *J. Org. Chem.* **2010**, *75*, 6035–6038.
- [25] L. J. Jiao, W. D. Pang, J. Y. Zhou, Y. Wei, X. L. Mu, G. F. Bai, E. H. Hao, *J. Org. Chem.* **2011**, *76*, 9988–9996.
- [26] V. Lakshmi, M. Ravikanth, *J. Org. Chem.* **2011**, *76*, 8466–8471.
- [27] S. H. Choi, K. Kim, J. Jeon, B. Meka, D. Bucella, K. Pang, S. Khatua, J. Lee, D. G. Churchill, *Inorg. Chem.* **2008**, *47*, 11071–11083.
- [28] M. J. Ortiz, A. R. Agarrabeitia, G. Duran-Sampedro, J. Bañuelos Prieto, T. A. Lopez, W. A. Massad, H. A. Montejano, N. A. Garcia, I. Lopez Arbeloa, *Tetrahedron* **2012**, *68*, 1153–1162.
- [29] K. Umezawa, A. Matsui, Y. Nakamura, D. Citterio, K. Suzuki, *Chem. Eur. J.* **2009**, *15*, 1096–1106.
- [30] S. G. Awuah, J. Polreis, V. Biradar, Y. You, *Org. Lett.* **2011**, *13*, 3884–3887.
- [31] X. D. Jiang, H. Zhang, Y. Zhang, W. Zhao, *Tetrahedron* **2012**, *68*, 9795–9801.
- [32] Y. Yang, Q. Guo, H. Chen, Z. Zhou, Z. Guo, Z. Shen, *Chem. Commun.* **2013**, *49*, 3940–3942.
- [33] T. Rohand, W. W. Qin, N. Boens, W. Dehaen, *Eur. J. Org. Chem.* **2006**, 4658–4663.
- [34] T. Rohand, M. Baruah, W. Qin, N. Boens, W. Dehaen, *Chem. Commun.* **2006**, 266–268.
- [35] Q. Bellier, F. Dalier, E. Jeanneau, O. Maury, C. Andraud, *New J. Chem.* **2012**, *36*, 768–773.

- [36] J. R. Lakowicz, *Principles of Fluorescence Spectroscopy*, 3rd ed., Springer, Singapore, **2006**.
- [37] A. B. Nepomnyashchii, S. Cho, P. J. Rossky, A. J. Bard, *J. Am. Chem. Soc.* **2010**, *132*, 17550–17559.
- [38] Gaussian 09, Revision A.1, M. J. Frisch, G. W. Trucks, H. B. Schlegel, G. E. Scuseria, M. A. Robb, J. R. Cheeseman, G. Scalmani, V. Barone, B. Mennucci, G. A. Petersson, H. Nakatsuji, M. Caricato, X. Li, H. P. Hratchian, A. F. Izmaylov, J. Bloino, G. Zheng, J. L. Sonnenberg, M. Hada, M. Ehara, K. Toyota, R. Fukuda, J. Hasegawa, M. Ishida, T. Nakajima, Y. Honda, O. Kitao, H. Nakai, T. Vreven, J. A. Montgomery, Jr., J. E. Peralta, F. Ogliaro, M. Bearpark, J. J. Heyd, E. Brothers, K. N. Kudin, V. N. Staroverov, R. Kobayashi, J. Normand, K. Raghavachari, A. Rendell, J. C. Burant, S. S. Iyengar, J. Tomasi, M. Cossi, N. Rega, J. M. Millam, M. Klene, J. E. Knox, J. B. Cross, V. Bakken, C. Adamo, J. Jaramillo, R. Gomperts, R. E. Stratmann, O. Yazyev, A. J. Austin, R. Cammi, C. Pomelli, J. W. Ochterski, R. L. Martin, K. Morokuma, V. G. Zakrzewski, G. A. Voth, P. Salvador, J. J. Dannenberg, S. Dapprich, A. D. Daniels, Ö. Farkas, J. B. Foresman, J. V. Ortiz, J. Cioslowski, D. J. Fox, Gaussian, Inc., Wallingford CT, **2009**.
- [39] A. D. Becke, *J. Chem. Phys.* **1993**, *98*, 5648–5652.
- [40] A. Gorman, J. Killoran, C. O'Shea, T. Kenna, W. M. Gallagher, D. F. O'Shea, *J. Am. Chem. Soc.* **2004**, *126*, 10619–10631.

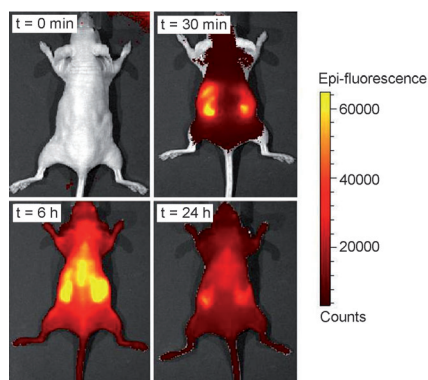
Received: June 28, 2013

Revised: July 18, 2013

Published online: ■ ■ ■, 0000

# FULL PAPER

**Something to PET:** We have rationally designed a versatile thieno-pyrrole-fused BODIPY intermediate useful for the development of near-infrared (NIR) multifunctional agents. The NIR excitation range is 650–840 nm. The agents produce bright fluorescence useful for biomedical imaging (see image), generate singlet oxygen (non-halogenated BODIPY) with decent fluorescence for dual therapy and imaging, and were functionalized with donor moieties to induce photoinduced electron transfer/internal charge transfer (PET/ICT).



## Fluorescent Probes

*Samuel G. Awuah, Sushanta K. Das,  
Francis D'Souza,  
Youngjae You\**



**Thieno-Pyrrole-Fused BODIPY Intermediate as a Platform to Multifunctional NIR Agents**

